Journal of Alloys and Compounds 509 (2011) 3623–3626

Contents lists available at ScienceDirect

Journal of Alloys and Compounds

journal homepage: www.elsevier.com/locate/jallcom

# Synthesis of $LiNi_{0.5}Mn_{1.5}O_4$ by solid-state reaction with improved electrochemical performance

X.Y. Feng, C. Shen, X. Fang, C.H. Chen*

*CAS Key Laboratory of Materials for Energy Conversions, Department of Materials Science and Engineering, University of Science and Technology of China, Anhui, Hefei 230026, China*

ARTICLE INFO

*Article history:*
Received 25 September 2010
Received in revised form
12 December 2010
Accepted 15 December 2010
Available online 22 December 2010

*Keywords:*
Lithium nickel manganese oxide
Cycling performance
Rate capability
Raman spectroscopy
Cyclic voltammetry

ABSTRACT

$LiNi_{0.5}Mn_{1.5}O_4$ spinel samples were synthesized by a two-step solid-state reaction method. Manganese acetate and nickel acetate were mixed together in a molar ratio of 3:1 and reacted at 500 °C to form a mixed Ni-Mn oxide, which reacted subsequently with lithium acetate at 900 °C to form a $LiNi_{0.5}Mn_{1.5}O_4$ powder. For comparison, manganese acetate, nickel acetate and lithium acetate were mixed together in a molar ratio of 3:1:2 and directly reacted in one-step at 900 °C. The $LiNi_{0.5}Mn_{1.5}O_4$ powder synthesized from the two-step process shows enhanced conductivity and improved rate performance. X-ray diffraction and Raman spectroscopy analyses indicate that the two-step sample has a space group of $Fd\bar{3}m$ while the one-step sample has a space group of $P4_332$. The cyclic voltammetry test has confirmed that lithium-ion cells with the two-step sample in the positive electrode exhibit lower impedance than those with the one-step sample.



## 1. Introduction

Recently, the interest in spinel-type $LiNi_{0.5}Mn_{1.5}O_4$ has increased substantially thanks in part to the successful application of $LiMn_2O_4$ spinel as the positive electrode material in high power lithium-ion batteries. In fact, this compound ($LiNi_{0.5}Mn_{1.5}O_4$) can be regarded as a special case of the doped compounds $LiMn_{2-y}M_yO_4$ where M is a transition metal element such as Cr [1,2], Co [2,3], Fe [4] and Cu [3]. The doped spinel compounds usually have a similar capacity of about 150 mAh $g^{-1}$ but differ a lot in their operating potentials. The new spinel cathode material $LiNi_{0.5}Mn_{1.5}O_4$ exhibits a high potential of about 4.7 V (versus Li) with a theoretical capacity of 146.7 mAh $g^{-1}$ [5–8]. Its cycling performance is better than that of $LiMn_2O_4$ which contains half of its manganese ions in the form of $Mn^{3+}$ that is mainly responsible for the capacity fading [9–12]. $LiNi_{0.5}Mn_{1.5}O_4$ also shows a non-negligible capacity fading because $LiNi_{0.5}Mn_{1.5}O_4$ synthesized at high temperatures often contains an impurity phase of $Li_xNi_{1-x}O_2$ ($x \approx 0.2$) or NiO [13,14]. The impurity comes from the loss of oxygen at high temperatures. The tetravalent manganese ($Mn^{4+}$) is unstable at high temperatures and can be converted to trivalent ($Mn^{3+}$) so that oxygen may partially evolve out of the lattice to form $LiNi_{0.5}Mn_{1.5}O_{4-x}$. When $x$ value becomes large, this phase becomes unstable and may decompose into two phases, i.e., $LiNi_{0.5-x}Mn_{1.5+x}O_{4-y}$ and $Li_xNi_{1-x}O_2$. To get rid of the impurity, an annealing process after the high temperature treatment is usually necessary. Amine et al. reported that after repeated annealing at 750 °C, the impurity phase disappears from the final product [15].

The $LiNi_{0.5}Mn_{1.5}O_4$ spinel has a good electronic conductivity because of the alterable oxidation state of nickel ion and manganese ion, especially when oxygen deficiency appears at high temperatures and its space group changes from $P4_332$ to $Fd\bar{3}m$. It is established that [16–19], the $Fd\bar{3}m$ phase is stable at high temperatures and has higher conductivity than the $P4_332$ phase, but it contains $Mn^{3+}$ ions that gives rise to a long charge/discharge plateau at 4.0 V. Which of the two phases is really formed is closely related to the preparation conditions. We have found in this study that a two-step solid-state reaction process leads to the formation of $Fd\bar{3}m$ phase with better electrochemical performance in comparison with the samples from one-step process.

## 2. Experimental

Spinel $LiNi_{0.5}Mn_{1.5}O_4$ samples were synthesized by a two-step solid-state reaction process. All chemicals were purchased from Sinopharm Chemical Reagent Co., Ltd. Nickel acetate ($Ni(Ac)_2{\cdot}4H_2O$, 10 mmol) and manganese acetate ($Mn(Ac)_2{\cdot}4H_2O$, 30 mmol) were mixed and grinded in a mortar. Then the mixtures were calcined in air to 500 °C in an alumina crucible at a rate of 3 °C $min^{-1}$. The calcination at 500 °C was held for 5 h followed by a natural cooling to room temperature so that mixed oxides of nickel and manganese were obtained. In order to find out how much lithium acetate ($LiAc{\cdot}2H_2O$) should be added later to form the spinel phases, we weighed the crucible (19.5405 g), the crucible and the acetate (28.8940 g) before the calcination, the crucible and the oxides (22.5296 g) after the calcination. Thus, the weight of the powder sample was retained by 31.96% after the calcination. Therefore, 0.7863 g of the thus-obtained mixed oxides of nickel and manganese correspond to

* Corresponding author. Tel.: +86 551 3606971; fax: +86 551 3601952.
*E-mail address:* cchchen@ustc.edu.cn (C.H. Chen).

0925-8388/$ – see front matter © 2010 Elsevier B.V. All rights reserved.
doi:10.1016/j.jallcom.2010.12.116

2.4603 g of acetates (2.5 mmol $Ni(Ac)_2{\cdot}4H_2O$ and 7.5 mmol $Mn(Ac)_2{\cdot}4H_2O$). Hence, 0.7863 g of mixed Ni-Mn oxides were mixed with 0.501 g (5 mmol) of $LiAc{\cdot}2H_2O$ to obtain a mixture with the Li:Ni:Mn molar ratios equal to 1:0.5:1.5. This mixture was first calcined at 500 °C for 5 h, then sintered at 900 °C for 10 h, and subsequently annealed at 700 °C for 10 h. For the sake of comparison, another contrast spinel sample was also prepared by a one-step method. Namely, nickel acetate, manganese acetate and lithium acetate were mixed together in the beginning, and then we followed the above second step procedure to synthesize a $LiNi_{0.5}Mn_{1.5}O_4$ powder.

The crystalline structures of the $LiNi_{0.5}Mn_{1.5}O_4$ samples were characterized by X-ray diffraction (XRD) using a diffractometer (Philips X'Pert Pro Super, Cu Kα radiation). The diffraction patterns were recorded at room temperature in the $2\theta$ range from 10° to 80°. To find out which space groups are for the $LiNi_{0.5}Mn_{1.5}O_4$ samples, Raman spectra of these two samples were measured at room temperature using a LABRAM-HR Confocal Laser Micro-Raman spectrometer equipped with an argon laser (wavelength 514.5 nm). Their morphology and particle size were characterized by scanning electron microscopy (JSM-6390LA, JEOL).

The electrochemical properties of the $LiNi_{0.5}Mn_{1.5}O_4$ samples were measured in the CR2032 coin-type half-cells $LiNi_{0.5}Mn_{1.5}O_4$/Li with 1 M $LiPF_6$ in EC:DMC (1:1, w/w) as the electrolyte. The positive electrode consisted of a mixture of 84 wt% $LiNi_{0.5}Mn_{1.5}O_4$, 8 wt% carbon black and 8 wt% PVDF binder. The cells were assembled in an argon-filled dry-box (MBraun Labmaster 130) with a porous polypropylene membrane (Celgard 2400) as the separator. They were cycled on a multi-channel battery test system (NEWARE BTS-610) in the mode of constant current followed by constant voltage (CC-CV) in the voltage range from 3.5 to 5.1 V. Also, cyclic voltammograms (CV) of the cells were measured at room temperature on a CHI 604 Electrochemical Workstation in the voltage range from 3.5 V to 5.1 V at the scanning rate of 0.2 mV $s^{-1}$.

## 3. Results and discussion

### 3.1. Structure and morphology of $LiNi_{0.5}Mn_{1.5}O_4$ powders

The X-ray diffraction patterns of the prepared $LiNi_{0.5}Mn_{1.5}O_4$ samples are shown in Fig. 1. They exhibit similar patterns that can be attributed to a cubic spinel structure of $LiNi_{0.5}Mn_{1.5}O_4$. Except for the diffraction peaks of $LiNi_{0.5}Mn_{1.5}O_4$, there is a small peak (marked with '*') around 45° that corresponds to an impurity phase of $Li_xNi_{1-x}O_2$, suggesting an oxygen loss reaction at high temperatures. Although the XRD patterns can confirm the formation of $LiNi_{0.5}Mn_{1.5}O_4$ spinel phases, there are two space groups, $Fd\bar{3}m$ and $P4_332$, of the $LiNi_{0.5}Mn_{1.5}O_4$ spinel which can be distinguished by their Raman spectra (Fig. 2). According to Julien et al.'s study [18], the two-step sample has the space group of $Fd\bar{3}m$ (Fig. 2), while the one-step sample has the space group of $P4_332$ (Fig. 2). In the $P4_332$ phase, $Ni^{2+}$ ions take the 4b sites and $Mn^{4+}$ ions take the 12d sites. On the other hand, in the $Fd\bar{3}m$ phase, both $Ni^{2+}$ and $Mn^{4+}$ ions take the 32e sites randomly. Considering their different synthesis procedures, the difference in the space groups may be related to their starting materials. Because the two-step sample uses mixed nickel and manganese oxides as the starting materials, the nickel oxide and manganese oxide are transformed from their well-mixed acetates. When they react further with lithium acetate to form the spinel $LiNi_{0.5}Mn_{1.5}O_4$ product, $Ni^{2+}$ and $Mn^{4+}$ ions are randomly distributed in 32e sites in the $Fd\bar{3}m$ lattice. As a comparison, for the one-step sample, when the lithium, nickel and manganese acetates are reacted from the beginning, $Ni^{2+}$ and $Mn^{4+}$ ions can take different sites in the crystal structure, i.e. $Ni^{2+}$ at 4b, $Mn^{4+}$ at 12d sites in the $P4_332$ lattice. Therefore, the mixability of $Ni^{2+}$ ions and $Mn^{4+}$ ions may result in structures with different space groups.

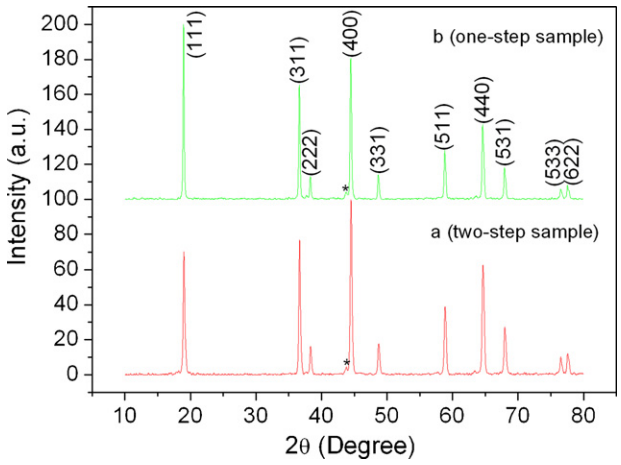


**Fig. 1.** XRD patterns of the $LiNi_{0.5}Mn_{1.5}O_4$ samples prepared by two-step (a) and one-step (b) solid-state reactions.

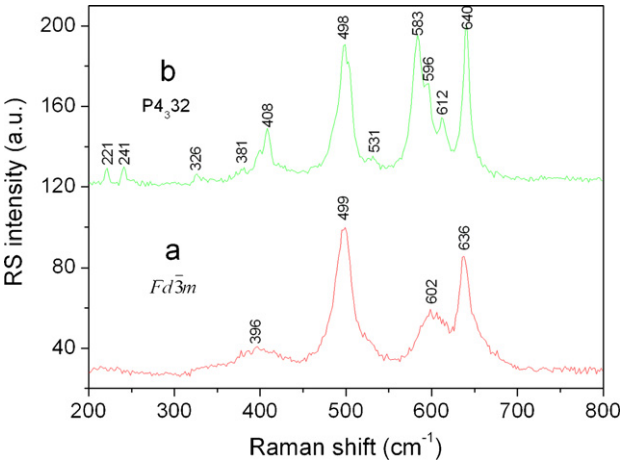


**Fig. 2.** Raman spectra of the $LiNi_{0.5}Mn_{1.5}O_4$ samples prepared by two-step (a) and one-step (b) solid-state reactions.

The scanning electron microscopy images of the samples are shown in Fig. 3. It can be seen that both one-step and two-step

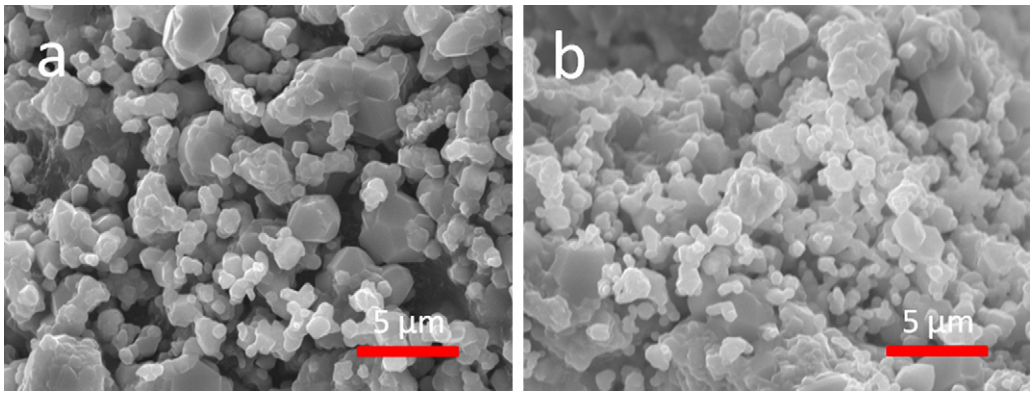


**Fig. 3.** SEM images of the $LiNi_{0.5}Mn_{1.5}O_4$ samples prepared by two-step (a) and one-step (b) solid-state reactions.

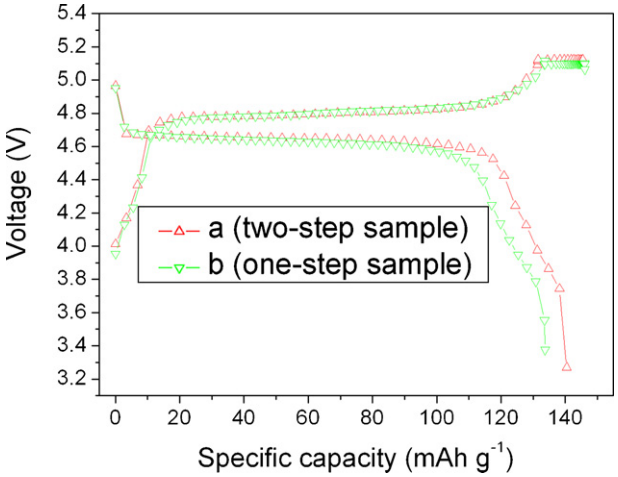


**Fig. 4.** Voltage profiles (4th cycle) of the $LiNi_{0.5}Mn_{1.5}O_4$ samples prepared by two-step (a) and one-step (b) solid-state reactions (charged and discharged at the current density of 150 mA $g^{-1}$).

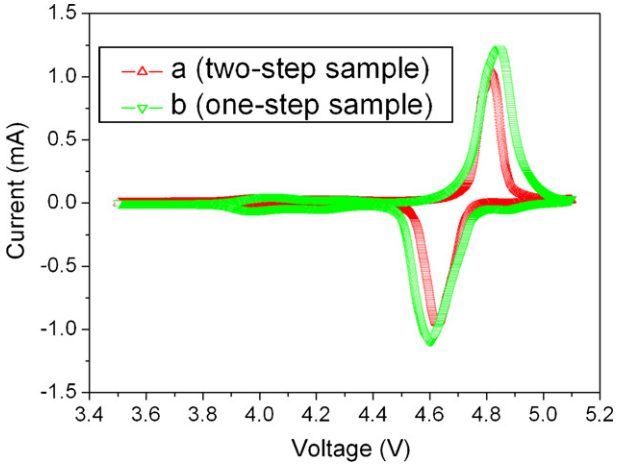


**Fig. 6.** Cyclic voltammograms of the $LiNi_{0.5}Mn_{1.5}O_4$ samples prepared by two-step (a) and one-step (b) solid-state reactions (the second cycle at the rate of 0.2 mV $s^{-1}$).

powders are composed of particles of similar sizes from 1 to 4 μm. The surface of these particles seems rather smooth. Therefore, the difference in conductivity between these two samples (see below) is due to the difference in their intrinsic structures, rather than due to any difference in the particle size.

### 3.2. Electrochemical performance of $LiNi_{0.5}Mn_{1.5}O_4$

The charge–discharge curves (4th cycle) of the as-synthesized samples measured at the current density of 150 mA $g^{-1}$ (or 1 C rate) are shown in Fig. 4. They give a plateau at 4.7 V and a slope between 4.7 V and 3.7 V. The plateau on the discharge curve corresponds to the conversion from $Ni^{4+}$ to $Ni^{2+}$ and the slope corresponds to the reaction from $Mn^{4+}$ to $Mn^{3+}$. Also, both samples show almost the same profile but the two-step sample has a higher capacity. Since the slope between 4.7 V and 3.7 V is related to the reaction from $Mn^{4+}$ to $Mn^{3+}$, the similar capacity (10–20 mAh $g^{-1}$) in the region of these two samples suggests the similar solubility of $Mn^{3+}$ in these two samples. Hence, the difference in the space groups of these two samples not only results in the oxygen loss at high temperature but also leads to difference in capacity due to the difference in the electronic conductivity.

Fig. 5 shows the cycling performance of the two samples. The two-step sample has a capacity of 140 mAh $g^{-1}$ at the 1st cycle and 135 mAh $g^{-1}$ after 100 cycles with approximately 0.05 mAh $g^{-1}$ capacity loss per cycle. The one-step sample has a capacity of 134 mAh $g^{-1}$ at the 1st cycle, and 121 mAh $g^{-1}$ retained after 80 cycles with approximately 0.16 mAh $g^{-1}$ capacity loss per cycle. Obviously, the two-step sample shows better cycling performance.

The cyclic voltammograms of two half-cells made with the two different $LiNi_{0.5}Mn_{1.5}O_4$ samples are shown in Fig. 6. Each of them has a small peak at 4.0 V and a strong peak at 4.6 V in the discharge step. As mentioned before, the two peaks correspond to the 4.6 V plateau and 4.0 V slope in the voltage profiles (Fig. 4). Since the voltage difference between the cathodic and anodic peaks is related to the impedance of the cells, which is about 0.195 V for the two-step sample and 0.243 V for the one-step samples, thus, it is obvious that the impedance of the two-step sample is less than that of the one-step sample.

The rate performance of the prepared samples is shown in Fig. 7. At the rate of 1 C, the two-step sample shows a capacity of about 140 mAh $g^{-1}$, which is about 5 mAh $g^{-1}$ higher than that of the one-step sample (135 mAh $g^{-1}$). When the C rate increases, the difference in capacity between these two samples also increases. The two-step sample can retain a capacity of about 113 mAh $g^{-1}$ at the rate of 10 C, which is 82% of its capacity at 1 C, while the one-step sample delivers only 93 mAh $g^{-1}$ at the rate of 10 C, which is 69% to its capacity at 1 C. Obviously, the rate performance of the two-step sample is better than that reported in literature [20,21]. When the

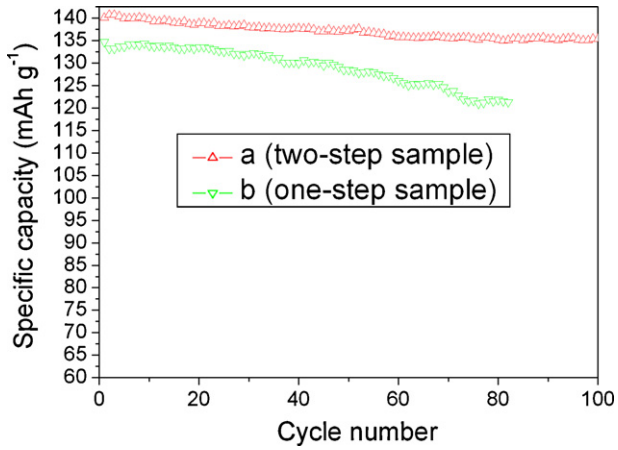


**Fig. 5.** Cycling performance of the $LiNi_{0.5}Mn_{1.5}O_4$ samples prepared by two-step (a) and one-step (b) solid-state reactions.

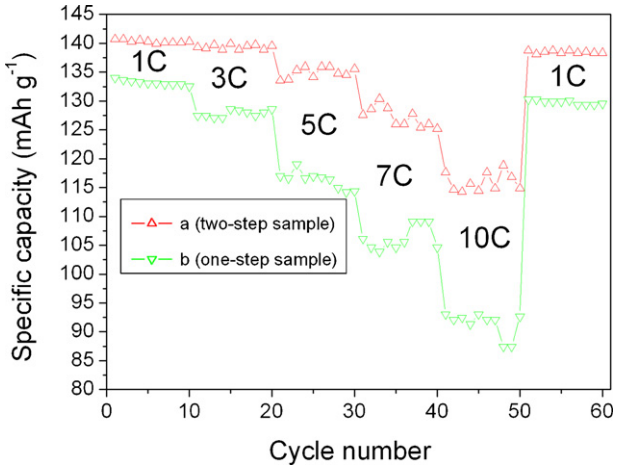


**Fig. 7.** Rate performance of the $LiNi_{0.5}Mn_{1.5}O_4$ samples prepared by two-step (a) and one-step (b) solid-state reactions.

rate goes back to 1 C, their specific capacities can roughly return to the initial levels for both samples, but the one-step sample shows more capacity fading due likely to its poorer cycling performance (Fig. 5).

## 4. Conclusions

$LiNi_{0.5}Mn_{1.5}O_4$ spinel powders of different space groups have been synthesized respectively by the one-step and two-step solid-state reaction processes. The difference in their space groups is found to be closely related to the mixability of $Ni^{2+}$ ions and $Mn^{4+}$ ions. In the two-step process, the good mixing of the two ions in the lattice leads to the formation of $LiNi_{0.5}Mn_{1.5}O_4$ with $Fd\bar{3}m$ symmetry. Otherwise, the $P4_332$ symmetry tends to be formed in the one-step process. Due to the difference in their crystal structures and electronic conductivity, the two-step sample shows better cycling stability and rate performance than the one-step sample, and is more suitable for commercial applications.

## Acknowledgments

This study was supported by National Science Foundation of China (grant no. 20971117 and 10979049) and Education Department of Anhui Province (grant no. KJ2009A142). We are also grateful to the Solar Energy Operation Plan of Academia Sinica.

## References

[1] R. Thirunakaran, A. Sivashanmugam, S. Gopukumar, C.W. Dunnill, D.H. Gregory, Mater. Res. Bull. 43 (2008) 2119.
[2] Y.P. Fu, Y.H. Su, S.H. Wu, C.H. Lin, J. Alloys Compd. 426 (2006) 228.
[3] P. Strobel, A.I. Palos, M. Anne, F.L. Cras, J. Mater. Chem. 10 (2000) 429.
[4] Q.H. Wu, J.M. Xu, Q.C. Zhuang, S.G. Sun, Solid State Ionics 177 (2006) 1483.
[5] S.H. Oh, S.H. Jeon, W.I. Cho, C.S. Kim, B.W. Cho, J. Alloys Compd. 452 (2008) 389.
[6] T.Y. Yang, K.N. Sun, Z.Y. Lei, N.Q. Zhang, Y. Lang, J. Alloys Compd. 502 (2010) 215.
[7] L. Zhang, X.Y. Lv, Y.X. Wen, F. Wang, H.F. Su, J. Alloys Compd. 480 (2009) 802.
[8] H.Y. Xu, S. Xie, N. Ding, B.L. Liu, Y. Shang, C.H. Chen, Electrochim. Acta 51 (2006) 4352.
[9] S. Hirose, T. Kodera, T. Ogihara, J. Alloys Compd. 506 (2010) 883.
[10] H. Sahan, H. GOktepe, S. Patat, A. Ulgen, Solid State Ionics 181 (2010) 1437.
[11] H. Kobayashia, H. Sakaebe, K. Komoto, H. Kageyama, M. Tabuchi, K. Tatsumia, T. Kohigashi, M. Yonemura, R. Kanno, T. Kamiyama, Solid State Ionics 156 (2003) 309.
[12] H. Sahan, H. Goktepe, S. Patat, A. Ulgen, Solid State Ionics 178 (2008) 1837.
[13] H.S. Fang, Z.X. Wang, X.H. Li, H.J. Guo, W.J. Peng, J. Power Sources 153 (2006) 174.
[14] Z.Y. Chen, H.L. Zhu, S. Ji, V. Linkov, J.L. Zhang, W. Zhu, J. Power Sources 189 (2009) 507.
[15] Q. Zhong, A. Bonakdarpour, M. Zhang, Y. Gao, J.R. Dahn, J. Electrochem. Soc. 144 (1997) 205.
[16] H.S. Huang, L.P. Li, G.S. Li, J. Power Sources 167 (2007) 223.
[17] N. Amdouni, K. Zaghib, F. Gendron, A. Mauger, C.M. Julien, Ionics 12 (2006) 117.
[18] C.M. Julien, F. Gendron, A. Amdounib, M. Massot, Mater. Sci. Eng. B 130 (2006) 41.
[19] J.H. Kim, S.T. Myung, C.S. Yoon, S.G. Kang, Y.K. Sun, Chem. Mater. 16 (2004) 906.
[20] D.C. Li, A. Ito, K. Kobayakawa, H. Noguchi, Y. Sato, Electrochim. Acta 52 (2007) 1919.
[21] T.F. Yi, X.G. Hu, J. Power Sources 167 (2007) 185.